Secondary Structure of the Pentraxin Female Protein in Water Determined by Infrared Spectroscopy: Effects of Calcium and Phosphorylcholine†

Aichun Dong,‡ Byron Caughey,*,§ Winslow S. Caughey,*,‡ Kolari S. Bhat,§ and John E. Coe§

Department of Biochemistry, Colorado State University, Fort Collins, Colorado 80523, and NIAID, National Institutes of Health, Rocky Mountain Laboratories, Hamilton, Montana 59840

Received February 6, 1992; Revised Manuscript Received July 17, 1992

ABSTRACT: The secondary structure of hamster female protein in aqueous solutions in the presence or absence of calcium and phosphorylcholine has been investigated using Fourier transform infrared spectroscopy. Our present studies provide the first evaluation of the secondary structure of FP and its calcium- and phosphorylcholine-dependent conformational changes. Quantitative analysis indicated that FP is composed of 50% β-sheet, 11% α-helix, 29% β-turn, and 10% random structures. Calcium- and phosphorylcholine-dependent infrared spectral changes were observed in regions assigned to β-sheet, α-helix, turn, and random structures. The infrared-based secondary structure compositions were used as constraints to compute theoretical locations for the different secondary structures along the amino acid sequence of the FP protein. Two putative calcium-binding sites were proposed for FP (residues 93–109 and 150–168) as well as other members of the pentraxin family on the basis of the theoretical secondary structure predictions and the similarity in sequence between the pentraxins and EF-hand calcium-binding proteins. The changes in protein conformation detected upon binding of calcium and phosphorylcholine provide a mechanism for the effects of these ligands on physiologically important properties of the protein, e.g., activation of complement and association with amyloids.

Female protein (FP),[1] C-reactive protein (CRP), and serum amyloid P component (SAP) belong to a family of proteins called pentraxins (Osmand et al., 1977; Coe et al., 1981). Pentraxins, named for their cyclic pentameric configuration of five noncovalently bound identical subunits (Osmand et al., 1977), are ancient proteins which have evolved at a conservative rate. *Limulus* CRP isolated from the hemolymph of horseshoe crab shares about 25% amino acid sequence identity with its mammalian counterparts (Nguyen et al., 1986a,b), whereas 71% sequence identity is shared by mouse CRP and human CRP (Woo et al., 1985; Whitehead et al., 1990). Hamster FP shares 50% and 72% sequence homology with human CPR and human SAP, respectively (Dowton & Holden, 1991). The evolutionary conservation of pentraxin genes and the ubiquitous presence of pentraxins in most higher organisms suggest an essential function for these proteins. Although a compelling reason for the existence of these proteins has not been found, pentraxins have been shown to be acute-phase proteins with a variety of Ca^{2+}-dependent binding activities (Gotschlich & Edelman, 1967; Coe, 1983; Coe & Ross, 1983; Painter et al., 1982). FP and CRP can bind phosphorylcholine (PC) and activate complement (Etlinger & Coe, 1986; Kaplan & Volanakis, 1974). FP and SAP have been identified as peripheral components of a variety of amyloids (Cathcart et al., 1965; Bladen et al., 1966; Coe & Ross, 1985), and it appears that the levels of FP expression can have a profound influence on amyloid formation in vivo (Coe & Ross, 1990).

Little is known about the secondary structures of pentraxins; however, analysis of human CRP by circular dichroism (Young & Williams, 1978) and monoclonal antibodies (Kilpatrick et al., 1982) provided estimates of the β-sheet and α-helix content and indicated a small conformational change occurred with Ca^{2+} binding. In the present study, we investigated the secondary structure of FP and its Ca^{2+}- and PC-dependent conformational changes using a recently developed Fourier transform infrared (FT-IR) spectroscopy technique that allows the secondary structure analysis of proteins in aqueous media. The amide I region of protein infrared spectra contains strong absorption bands due almost entirely to the carbonyl stretch vibration of the peptide backbone (Miyazawa & Blout, 1961; Krimm & Bandekar, 1986; Byler & Susi, 1986). The frequencies of these bands are sensitive to the secondary structure of proteins (Koenig & Tabb, 1980; Byler & Susi, 1986). Empirical studies have shown that the infrared amide I band areas associated with a particular secondary structure (e.g., α-helix, β-sheet, turn, and random structures), divided by the sum of all band areas assigned to secondary structures, provide a quantitative estimation of the relative amounts of the secondary structure components which are close to those derived from X-ray diffraction data (Byler & Susi, 1986; Dong et al., 1990). Our analysis indicates that FP is predominantly composed of β-sheet and turn, with smaller amounts of α-helix and random structures. Ca^{2+}-dependent conformational changes were detected in almost all structural regions, especially the β-sheet region. Addition of PC caused further structural changes. A theoretical prediction of the locations for different types of secondary structures in FP was carried out on the basis of knowledge of the infrared-based secondary structure composition. The locations of the two putative Ca^{2+}-binding sites in FP and other members of the pentraxin family are proposed.

† This work was supported in part by Colorado Agricultural Experiment Station Project 643 and by a gift from Strohtech, Inc.

* To whom correspondence should be addressed.

‡ Colorado State University.

§ Rocky Mountain Laboratories.

[1] Abbreviations: FP, female protein; FT-IR, Fourier transform infrared; IR-SD, infrared second derivative; CRP, C-reactive protein; SAP, serum amyloid P component; PC, phosphorylcholine.

0006-2960/92/0431-9364$03.00/0

MATERIALS AND METHODS

Sample Preparation. Random-bred Syrian hamsters (*Mesocricetus auratus*) were obtained from the animal facilities of the Rocky Mountain Laboratories. Syrian hamster FP was isolated from normal serum by Ca^{2+}-dependent binding to a PC–Sepharose column and elution with free PC (0.001 M) followed by extensive dialysis as previously described (Coe et al., 1981). Ca^{2+}-depleted FP was obtained by dialysis against 10 mM Tris-HCl/140 mM NaCl/1 mM EGTA for 24 h; then EGTA was removed by further dialysis against buffer without EGTA. For infrared measurements, FP (15 mg/mL) was dissolved in 10 mM Tris-HCl/140 mM NaCl, pH 8.0, with or without $CaCl_2$, $MgCl_2$, PC, or EDTA as described under Results.

Infrared Spectra Measurement. The infrared spectra of FP were measured at 20 °C with a Perkin-Elmer Model 1800 FT-IR spectrophotometer equipped with a Hg/Cd/Te detector. FP solutions were prepared for infrared measurement in a Beckman FH-01 cell with CaF_2 windows and a 6-μm path-length spacer. Spectral measurements and analysis follow the criteria and double-subtraction procedure of Dong et al. (1990, 1992) with minor modification. The factoring of water vapor subtraction was based on the elimination of water vapor bands outside the amide I region between 1850 and 1720 cm^{-1} which resulted in a featureless base line in this region of the second-derivative spectrum. The intrinsically overlapped amide I band contour was subjected to resolution enhancement using a second-derivative calculation. The secondary structure composition was determined by second-derivative/curve-fitting analysis using Spectra Calc software (Galactic Industries Corp.) on a 386-based personal computer. The inverted second-derivative spectra were obtained by factoring by −1 and were fitted with Gaussian band profiles. Initial band positions were taken directly from the second-derivative spectra, and no additional band was added. During the curve-fitting process, the heights, widths, and positions of all bands were varied simutaneously. The relative integrated intensity of each band was then calculated from final fitted band heights and widths.

Theoretical Analysis of Female Protein Structure. Analysis of the protein structure was carried out by using previously described algorithms (Garnier et al., 1978) with the aid of PC-Gene (Intelligenetics, Mountain View, CA) and Sequence Analysis Package (Genetics Computer Group, Inc., Madison, WI). For these analyses, Convex 240 and IBM PS/2 computers were used. The decision constants employed in the Garnier secondary structure prediction for α-helix, β-sheet, turn, and random coil were 20, −125, −55, and 0, respectively.

RESULTS

Infrared Spectra of FP. The primary infrared spectra of FP (15 mg/mL) in 10 mM Tris-HCl/140 mM NaCl, pH 8.0, with or without 2 mM $CaCl_2$ or 2 mM $CaCl_2$ plus 1 mM PC in the region 1900–1200 cm^{-1} are shown in Figure 1. The spectra conform to the criteria established earlier for subtraction of the spectrum due to liquid and gaseous water from the observed protein spectrum (Dong et al., 1990, 1992). The spectra of FP exhibit absorbance maxima for amide I, amide II, and amide III bands near 1634, 1550, and 1250 cm^{-1}, respectively. It has been well documented that the position of the infrared amide I band is determined by the predominant secondary structure in the proteins (Miyazawa & Blout, 1960; Koenig & Tabb, 1980; Krimm & Bandekar, 1986; Byler & Susi, 1986). Recently, we have studied 26 globular proteins

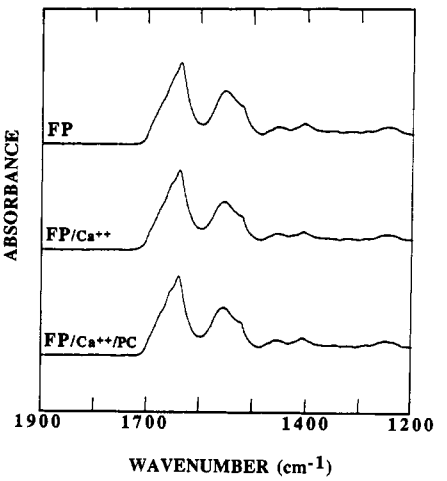

FIGURE 1: Infrared spectra of hamster female protein in water solutions with or without calcium and phosphorycholine. The contributions of the buffer and water vapor have been substracted from the primary spectra. The FP was at a concentration of 15 mg/mL in 10 mM Tris-HCl/140 mM NaCl, pH 8.0, with or without 2 mM $CaCl_2$ or 2 mM $CaCl_2$ plus 1 mM PC.

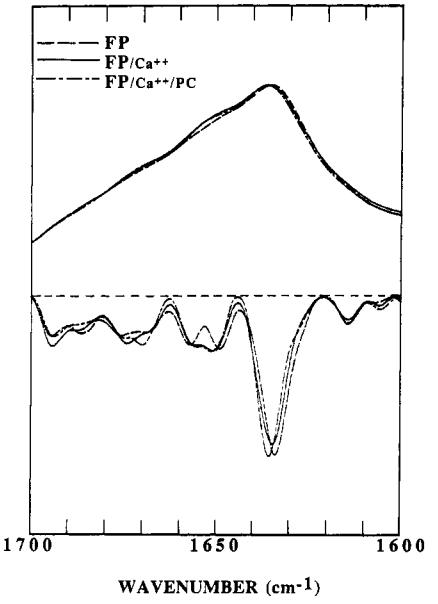

FIGURE 2: Primary and second-derivative amide I infrared spectra of hamster female protein in water solutions. FP (– –) and FP with Ca^{2+} (—) or with Ca^{2+} plus PC (–·–). (Top) Primary spectra. (Bottom) Second-derivative spectra. The second-derivative spectra of FP shown here were confirmed by at least two independently isolated protein samples.

with widely varying secondary structure compositions in H_2O-based solutions and found that the maximum absorbance of the amide I band of proteins with predominant α-helix will occur near 1656 ± 2 cm^{-1} and those with predominant β-sheet structure will be found between 1643 and 1631 cm^{-1} (A. Dong, P. Huang, B. Caughey, and W. S. Caughey, unpublished results). The primary spectra of FP exhibited a maximum amide I absorbance near 1634 cm^{-1} which indicated a predominance of β-sheet structure in this protein.

Second-Derivative Analysis of FP Infrared Spectra. To further resolve the overlapping bands within the amide I band contour and quantitate the secondary structure components of FP, second-derivative analyses of the spectra were carried out. Absorbance bands in the primary spectra were revealed as negative bands in the derivative spectra. Figure 2 presents an overlay of primary and second-derivative amide I spectra of FP with or without Ca^{2+} and PC. Significant spectral

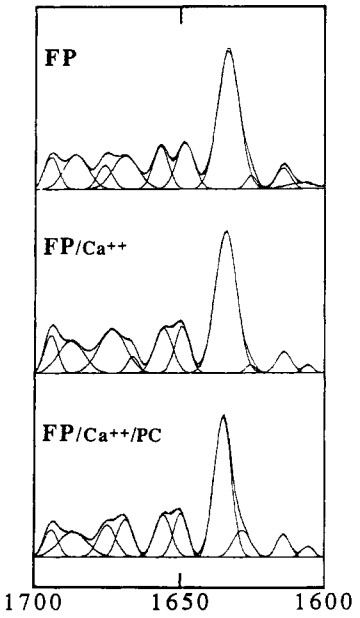

FIGURE 3: Curve-fitting of inverted second-derivative spectra of FP with or without Ca^{2+} and PC.

Table I: Secondary Structures of Hamster Female Protein in Water As Determined by Amide I Infrared Second-Derivative Analysis[a]

	secondary structure (%)			
female protein	α-helix	β-sheet	turn	random
Ca^{2+}-depleted	9.2	50.8	28.4	11.6
2 mM Ca^{2+}	10.8	50.0	29.8	9.4
2 mM Ca^{2+}/PC	10.8	50.9	28.9	9.4

[a] The values represent the percentage of the total integrated intensity of the second-derivative amide I spectral bands which corresponds to bands assigned to the designated secondary structure, and each value is the average of two or three independent determinations. By comparing IR-SD-derived secondary structure compositions of 26 proteins with those derived from X-ray crystallography, we have determined that the standard errors for the accuracy of our refined IR-SD method are 2.5% for helices (α-helix and distorted α-helix), 3.1% for β-sheet, 4.0% for reverse turns, and 3.6% for random structure (A. Dong, P. Huang, B. Caughey, and W. S. Caughey, unpublished results).

changes resulting from the addition of Ca^{2+} and PC to FP were revealed in both the primary and second-derivative spectra. Second-derivative analysis has also revealed bands ascribed to β-sheet (1694, 1634, and 1626 cm^{-1}), α-helix (1657 cm^{-1}), turn (1686, 1676, and 1669 cm^{-1}), and random structure (1649 cm^{-1}) (Gorga et al., 1989; Dong et al., 1990). Quantitative analysis (Figure 3) confirmed that the predominant secondary structure is β-sheet. Turn, α-helix, and random structures were observed in lower amounts (Table I).

The multiple bands in the β-sheet and turn regions of the second-derivative FP spectra indicated the presence of more than one subtype of these structures. Although, on theoretical grounds (Krimm & Bandekar, 1986), the high wavenumber β-structure-related band at 1694 cm^{-1} is thought to be specific for antiparallel β-sheet, the exact correspondence between β-structure-related bands and particular β-structure folding patterns as revealed by X-ray crystal structures has not yet been solidly confirmed (Susi & Byler, 1987). Data pertaining to the detailed assignment for various types of turn structure are also limited at the present time.

The potential interference from side-chain vibrations of amino acid residues such as Asn, Gln, Arg, and Lys and from

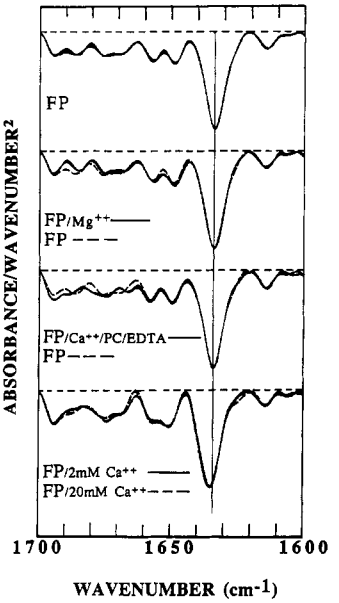

FIGURE 4: Comparisons of the second-derivative spectra of FP obtained under various conditions. The spectral reproducibility is supported by the superimposible second-derivative spectra obtained from different protein isolations and infrared measurements.

N-acetylglucosamine with secondary structure estimation utilizing the infrared amide I spectrum has been discussed in our previous reports (Caughey et al., 1991; Dong et al., 1992). The presence of N-linked glycan in FP has been shown in recent studies, and *N*-acetylglucosamine content has been estimated to be ≤5 residues per FP monomer (J. A. Sogn and J. E. Coe, unpublished data). FP also contains 6.1% Asn, 6.1% Lys, 4.2% Gln, and 3.3% Arg, respectively (Coe et al., 1981; Dowton et al., 1985). However, on the basis of the molar integrated intensity of *N*-acetylglucosamine residues and amino acid side chains determined previously (Caughey et al., 1991; Dong et al., 1992; Venyaminov & Kalnin, 1990), the contributions to the infrared amide I spectrum of FP from these groups are estimated to have an insignificant effect on the secondary structure composition we have determined.

Ca^{2+}-Dependent Secondary Structure Changes in FP. By comparison of the second-derivative spectra of FP with or without Ca^{2+} (Figures 2 and 3), Ca^{2+}-dependent spectral changes in regions assigned to β-sheet, random, α-helix, and turn structure were consistently seen which provided evidence for a conformational change due to Ca^{2+} binding to the protein. For Ca^{2+}-depleted FP, the β-sheet structure was represented by a strong band at 1633 cm^{-1} and two weaker bands at 1694 and 1626 cm^{-1}, and the α-helix and random structures were represented by bands at 1657 and 1649 cm^{-1}, respectively (Figures 2 and 3). Upon the addition of 2 mM Ca^{2+} (approximate serum concentration), the major β-structure-related band at 1633 cm^{-1} was shifted to 1634 cm^{-1}, which was accompanied by a small intensity decrease of the 1634-cm^{-1} band and an increase of the 1694-cm^{-1} band. Meanwhile, the bands assigned to α-helix and random structures shifted toward each other. No further significant spectral change was observed with a further 10-fold increase in the Ca^{2+} concentration, indicating that the Ca^{2+}-binding sites responsible for the Ca^{2+}-induced spectral changes were saturated at 2 mM (Figure 4). A similar spectrum was also obtained from FP purified with Ca^{2+}, and the addition of 2 mM EDTA caused the second-derivative spectrum to change to one like that of Ca^{2+}-depleted FP (data not shown). As a test of the divalent cation specificity of the Ca^{2+}-induced spectral changes, we added 2 mM $MgCl_2$ to the Ca^{2+}-depleted

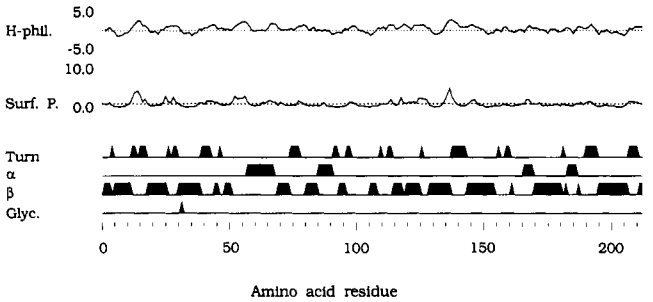

FIGURE 5: Hamster female protein secondary structure predictions by the method of Garnier et al. (1978) as constrained by the infrared-derived secondary structure compositions. Under the constraint of the chosen decision constants, 50.2% β-sheet, 12.3% α-helix, 21.3% turn, and 16.1% random structures were predicted from the FP amino acid sequence. The predicted locations of β-sheet (β), α-helices (α), and turn (Turn) thoughout the amino acid sequence of FP are shown relative to the hydrophicity (H-phil.) and log surface probability (Surf. P.) of residues.

FP, but little spectral change was observed (Figure 4). Thus, Mg^{2+} could not be substituted for Ca^{2+} to produce the same spectral effects.

Phosphorylcholine-Dependent Secondary Structure Changes in FP. Further spectral changes in the amide I region were observed by the addition of PC in the presence of Ca^{2+}, which shifted the major β-structure-related band further to 1635 cm^{-1}. Meanwhile, the band at 1626 cm^{-1} was shifted to 1628 cm^{-1} and increased in intensity (Figures 2 and 3). These observed effects of PC were dependent upon the presence of Ca^{2+} since such spectral changes were canceled in the presence of EDTA, a Ca^{2+} chelater (Figure 4).

Theoretical Locations of Secondary Structures. Having determined the secondary structure composition of FP by second-derivative infrared analysis (Table I), we obtained predictions of the location of these secondary structures using the alogrithm of Garnier and co-workers (Garnier et al., 1978). The infrared-based secondary structure compositions in Table I were used to constrain the Garnier predictions. This was done by choosing Garnier decision constants for each individual secondary structure component of FP which corresponded to the average of decision constants derived previously for other proteins containing similar amounts of that particular structure (Garnier et al., 1978). Under the constraint of the chosen decision constants, the Garnier method predicted a composition of 50.2% β-sheet, 12.3% α-helix, 21.3% turn, and 16.1% random structures from the FP amino acid sequence. The predicted locations of β-sheet, α-helix, and turn structures are shown in comparison to FP hydropathy and surface probability plots in Figure 5. Eleven strands of β-sheet containing 3–10 amino acid residues and 4 strands of α-helix containing 4–12 amino acid residues were predicted.

DISCUSSION

Spectral Reproducibility. The double-subtraction procedure described in our earlier study (Dong et al., 1992) has proven very effective for obtaining high-quality primary infrared spectra which, in turn, give highly reproducible second-derivative spectra. The high reproducibility of the second-derivative spectra is also shown in our present study. For example, the superimposible second-derivative spectra presented in Figure 4 were calculated from the primary spectra obtained from at least two independently isolated protein samples. As we have shown in studies of cytochrome *c* (Dong et al., 1992), the utilization of the double-subtraction procedure in protein infrared spectroscopic investigations has enabled us to monitor smaller protein conformational changes than was possible previously. Using this technique, we established that FP consists predominantly of β-sheet structure and provided direct spectroscopic evidence for conformational changes induced by the binding of Ca^{2+} and PC.

Comparison of Secondary Structures of FP and Other Pentraxins. Comparative studies on secondary structures of FP, CRP, and SAP have not been conducted. However, using far-UV CD spectroscopy, Young and Williams (1978) have reported that human CRP consists of 45% β-sheet and 34% α-helix and human SAP exhibits a CD spectrum similar to that of CRP. The content of β-sheet structure estimated for CRP is very similar to the 50% β-sheet structure estimated for FP, which supports the idea that pentraxins have similar secondary structure folding patterns. The estimated α-helical content of CRP is somewhat higher than that estimated for FP, and no information about the turn and random structures for CRP was given. CD spectroscopy is one of the widely used techniques for studying protein conformation (Greenfield & Fasman, 1969; Chen et al., 1972; Brahms & Brahms, 1980; Provencher & Glockner, 1981; Hennessey & Johnson, 1981; Johnson, 1990). It is known to be very sensitive to α-helical structure and less sensitive to β-sheet, turn, and random structures of proteins. However, the advantage of CD spectroscopy in estimating α-helical structure can be offset by the contribution from aromatic amino acid side chains in the far-UV region, especially when aromatic side-chain clusters are formed in the protein (Hooker & Schellman, 1970; Manning & Woody, 1989). The amino acid composition of human CRP derived from the complementary DNA sequence shows that it contains 8 Tyr, 13 Phe, and 6 Trp (Liu et al., 1982; Woo et al., 1985). The location of many of these residues sequentially close to each other suggests they may form aromatic side-chain clusters to result in an overestimate of the α-helix structure for CRP by use of far-UV CD spectroscopy.

Ca^{2+}- and PC-Dependent Conformational Changes. The Ca^{2+}-dependent binding properties of pentraxins suggest that there might be Ca^{2+}-dependent conformational changes in this group of proteins. Such a Ca^{2+}-dependent conformational change has been observed in human CRP (Young & Williams, 1978; Kilpatrick et al., 1982). Since Ca^{2+} is essential for binding of PC to human CRP and FP (Gotschlich & Edelman, 1967; Volanakis & Kearney, 1981; Coe et al., 1981), it has been suggested that Ca^{2+} acts as an allosteric effector which induces the proper conformation of the PC-binding site of CRP (Volanakis & Kearney, 1981). Our infrared data indicating that removal of Ca^{2+} from FP causes marked changes in both the Ca^{2+}- and PC-related secondary structure folding patterns are consistent with this view. These secondary structure changes were detected mainly in β-sheet and turn structural regions, suggesting that the Ca^{2+}-binding site of FP is located in regions containing both β-sheet and turn structures or is affected allosterically by the binding of Ca^{2+} to a more distant site. Further characterization of the spacial distribution of the Ca^{2+}-binding site(s) of FP and the potential allosteric interactions may provide information about the function of this ancient family of proteins. By binding PC in the presence of Ca^{2+}, FP is known to be capable of activating the complement system (Etlinger & Coe, 1986). Presumably, the subtle but definite spectral change seen by IR after addition of PC to FP in the presence of Ca^{2+} represents the conformational alteration in FP needed for triggering complement

Table II: Amino Acid Sequences and Secondary Structures of the First Putative Ca^{2+}-Binding Site of Pentraxins Aligned with Known EF-Hand Ca^{2+}-Binding Loops of Parvalbumin and Galactose-Binding Protein (GBP)[a]

protein	starting residue	1 X	*	2	3 Y	4	5 Z	6 G	7 –Y	8	9 –X	10	11	*	12 –Z		ending residue
hamster FP[b]	94	T	S	W	E	S	S	S	G	I	A	E	F	W	V	N	G	109
mouse SAP[c]	96	T	T	W	E	S	S	S	G	I	V	E	F	W	V	N	G	111
human SAP[d]	96	V	S	W	E	S	S	S	G	I	A	E	F	W	I	N	G	111
Limulus CRP 1.1[e]	102	H	T	W	S	S	W	E	G	E	A	T	I	A	V	D	G	117
Limulus CRP 1.4	102	H	T	W	S	S	W	E	G	E	A	T	I	G	V	D	G	117
Limulus CRP 3.3	102	H	T	W	S	S	W	E	G	E	A	T	I	A	V	D	G	117
hamster CRP[f]	98	A	S	W	E	S	A	T	G	I	A	E	L	W	V	D	G	113
mouse CRP[g]	98	A	S	W	E	S	A	T	G	I	V	E	F	W	I	D	G	113
rabbit CRP[h]	98	A	S	W	E	S	S	T	G	I	A	E	L	W	V	D	G	113
human CRP[i]	98	T	S	W	E	S	A	S	G	I	V	E	F	W	V	D	G	113
predicted secondary structure for FP[j]		β	β	t	t	r	r	r	r	r	r	r	β	β	β	β	β	
parvalbumin[k]	50	I	D	*	Q	D	K	S	G	F	I	E	E	D	*	E	L	63
	89	G	D	*	S	D	G	D	G	K	I	G	V	D	*	E	F	102
secondary structure from X-ray[j]		α	α		r	r	r	r	r	r	r	r	α	α		α	α	
GBP[l]	133	Y	D	*	L	N	K	D	G	Q	I	Q	F	V^{144}	I^{204}	E	V	206
secondary structure from X-ray[j]		t	r		r	r	r	r	r	r	r	r	β	β	β	β	β	

[a] The amino acid residues are represented by the single-letter code. X, Y, Z, –X, and –Z refer to positions containing either D, N, E, Q, T, and S, which are highly conserved among EF-hand Ca^{2+}-binding proteins. The side-chain oxygen atoms of these residues provide Ca^{2+} coordinating ligands. The residue at position –Y provides its peptide carbonyl oxygen atom as the Ca^{2+} coordinating ligand (Vyas et al., 1987). Asterisks represent a position where one amino acid residue is inserted in pentraxins. [b] Dowton et al. (1985). [c] Mole et al. (1988); Whitehead & Rits (1989). [d] Mantzouranis et al. (1985). [e] Nguyen et al. (1986a,b). [f] Dowton & Holden (1991). [g] Whitehead et al. (1990). [h] Hu et al. (1986). [i] Oliveira et al. (1979); Woo et al. (1985). [j] β, β-sheet, t, turn; α, α-helix; r, random. [k] Coffee & Bradshaw (1973); Kretsinger & Nockolds (1973). [l] Mahoney et al. (1981); Vyas et al. (1987).

Table III: Amino Acid Sequences and Secondary Structures of the Second Putative Ca^{2+}-Binding Site of Pentraxins Aligned with Known EF-Hand Ca^{2+}-Binding Loops of Parvalbumin and Galactose-Binding Protein (GBP)[a]

protein	starting residue	1 X	2	3 Y	4	*	5 Z	6 G	7 –Y	8	9 –X	10	11	12 –Z		ending residue
hamster FP[b]	154	G	D	R	N	M	W	D	S	V	L	T	P	E	E	I	168
mouse SAP[c]	155	S	D	L	Y	M	W	D	Y	V	L	T	P	Q	D	I	169
human SAP[d]	155	G	D	L	Y	M	W	D	S	V	L	P	P	E	N	I	169
Limulus CRP 1.1[e]	160	G	E	L	S	E	L	N	L	W	N	T	V	L	N	H	174
Limulus CRP 1.4	160	G	E	L	S	E	L	N	L	W	N	T	V	L	N	H	174
Limulus CRP 3.3	160	G	E	L	S	E	L	N	L	W	N	T	V	L	N	H	174
hamster CRP[f]	157	G	D	V	N	M	W	D	I	V	L	S	P	E	Q	I	171
mouse CRP[g]	157	G	D	V	N	M	W	D	F	V	L	S	P	E	Q	I	171
rabbit CRP[h]	157	G	N	V	N	M	W	D	Y	A	L	S	P	E	E	I	171
human CRP[i]	157	G	N	V	N	M	W	D	F	V	L	S	P	D	E	I	171
predicted secondary structure for FP[j]		r	t	r	r	t	t	r	r	r	r	r	α	α	α	α	
parvalbumin[k]	50	I	D	Q	D	K	*	S	G	F	I	E	E	D	E	L	63
	89	G	D	S	D	G	*	D	G	K	I	G	V	D	E	F	102
secondary structure from X-ray[j]		α	α	r	r	r		r	r	r	r	r	α	α	α	α	
GBP[l]	133	Y	D	L	N	K	*	D	G	Q	I	Q	F^{143}	I^{204}	E	V	206
secondary structure from X-ray[j]		t	r	r	r	r		r	r	r	r	r	β	β	β	β	

[a] The amino acid residues are represented by the single-letter code. Asterisks represent a position where one amino acid residue is inserted in pentraxins. All footnotes are the same as in Table II.

activation. Circular dichroism studies of CRP failed to detect a conformational change related to PC binding (Young & Williams, 1978). Thus, CRP and FP may differ in their conformational response to PC binding. On the other hand, it is possible that the CD technique, being less sensitive to β-sheet and turn structures, may have been unable to detect subtle PC-induced changes in CRP.

Prediction of Ca^{2+}-Binding Sites of FP. Due to the apparent structural and functional importance of Ca^{2+} binding in FP and the other pentraxins, we attempted to localize the possible binding site(s) in FP. We sought sites in FP that (1) resembled the recognized consensus pattern of amino acid residues in EF-hand Ca^{2+}-binding domains (designated after the E and F helix of parvalbumin) of other proteins (Kretsinger, 1980; Kretsinger et al., 1991), (2) were conserved in other pentraxins, and (3) were predicted to contain the expected random (or loop) secondary structure that generally forms the core of such domains. Two loop-containing sites, namely, residues 93–109 and 150–168, were identified that contained primary sequences largely consistent with the consensus motif required for Ca^{2+} binding in parvalbumin and related molecules (Coffee & Bradshaw, 1973; Kretsinger & Nockolds, 1973; Kretsinger, 1980; Dang et al., 1985), and these motifs were also present in the other pentraxins (SAPs and CRPs) (Tables II and III). However, as shown by the alignment of the pentraxin sequences with the known EF-hand Ca^{2+}-binding loops of parvalbumin and galactose-binding protein (Tables II and III), there are 2 amino acid insertions in the segment corresponding to FP residues 94–109 between positions 1 and 2 and 11 and 12 of the typical EF-hand loop sequence, and 1 amino acid insertion in the segment containing FP residues 154–168 between the EF-hand loop positions 4 and 5. Such insertions have been correlated with lower affinity Ca^{2+}-binding sites (Kretsinger et al., 1991). Although the number and affinity of the Ca^{2+}-binding sites in FP have not been established, equilibrium dialysis studies of human CRP have indicated that it has two relatively low-affinity sites with K_d's of $\sim 6 \times 10^{-5}$ M (Kinoshita et al., 1989). The typical EF-hand Ca^{2+}-binding domain contains a helix–loop–helix conformation, but there is not strict adherence to this arrangement as shown in case of galatose-binding protein which has an α-helix–loop–β-sheet conformation (Vyas et al., 1987). Thus, the β-strands

predicted to flank the loops in the FP segments 93–109 and 150–168 should not necessarily disqualify these sites as Ca^{2+}-binding domains. On the basis of these considerations of predicted secondary structure, conformity of the primary sequence to the EF-hand Ca^{2+}-binding motif, and conservation of the primary sequence motif among all the pentraxins, we conclude that residues 93–109 and 150–168 are most likely to be the Ca^{2+}-binding domains of FP.

Kilpatrick et al. (1982) found that the Ca^{2+}-dependent binding of three anti-CRP monoclonal antibodies to human CRP was inhibited by the presence of PC and concluded that the PC-binding site of CRP might be at or near the Ca^{2+}-induced conformational epitope(s), but the Ca^{2+}-binding site was not located. Nguyen and co-workers (Nguyen et al., 1986a,b), comparing the primary sequences of *Limulus* CRP and human CRP, have found two highly conservative regions between the two proteins. The first conserved region corresponding most closely to FP residues 49–63 has been suggested to be involved in the binding of PC ligand (Liu et al., 1982; Nguyen et al., 1986a). The second conserved region corresponding to FP residues 136–147 was proposed to be involved in the Ca^{2+}-binding function of CRPs based on the sequence similarity between this CRP region and the Ca^{2+}-binding site of calmodulin and related molecules (Nguyen et al., 1986a). Furthermore, it was shown that proteolytic cleavage in the region could abrogate Ca^{2+}-binding activity (Kinoshita et al., 1989). It is interesting to note that the corresponding segment in FP has a predicted β-strand–turn–β-strand conformation with high potential of surface exposure (Figure 5). Therefore, the susceptibility of this particular region to protease is easily understood. However, two considerations argue against this being a most favorable candidate for the Ca^{2+}-binding site of FP or pentraxins generally. First, some important Ca^{2+} coordinate ligands [positions 5(Z) and 9($-X$) of CRP and 9($-X$) of FP] were occupied by a Phe residue (Kinoshita et al., 1989). The Phe residue does not have a side-chain oxygen atom to provide a coordinate ligand for Ca^{2+} and has a large hydrophobic side chain which could prevent a water molecule from providing an alternative oxygen ligand. Second, our secondary structure prediction for FP suggests that the potential conformation for this region is a rigid turn structure rather than the more flexible random structure. This may limit its ability to utilize the amide carboxyl groups of Phe residues at positions 5(Z) and 9($-X$) to serve as alternative Ca^{2+} ligands. In other words, the requirement of a loop conformation for Ca^{2+} binding (Kretsinger & Nockolds, 1973; Vyas et al., 1987) may not be satisfied, at least in FP. Thus, for this reason, we favor the segments identified in Tables II and III as the most likely Ca^{2+}-binding sites in FP and other pentraxins. However, we note these segments also have characteristics, namely, extra residue insertions which flank the loop sequence, which deviate from the classic consensus helix–loop–helix EF-hand Ca^{2+}-binding site.

Most EF-hand Ca^{2+}-binding proteins contain predominant α-helical structure (50–60%) (Kretsinger & Nockolds, 1973; Dang et al., 1985) in contrast to the dominant β-sheet structure (45–50%) found in the prentraxins that have been analyzed (Table I; Young & Williams, 1978). As serum proteins, however, pentraxins function in an environment containing a much higher concentration of Ca^{2+} than that found in intracellular environments where the typical EF-hand Ca^{2+}-binding proteins are found. Thus, like human CRP, pentraxins in general can be expected to have lower affinity for calcium than the intracellular calcium-binding proteins. Thus, structural deviations in the Ca^{2+}-binding sites of pentraxins from those of EF-hand loops might be tolerated. On the basis of the theoretical secondary structure prediction for FP, we suggest the Ca^{2+}-binding sites of pentraxins involve β-strand–loop–β-strand or β-strand–loop–α-helix conformations (Figure 5). These sites may be similar to the site in galactose-binding protein (Vyas et al., 1987, 1991) or concanavalin A (Kalb & Levitzki, 1968; McPhalen et al., 1991) where a β-sheet secondary structure has been found in the Ca^{2+}-binding domain.

ACKNOWLEDGMENT

We are most grateful to Mary J. Ross for technical assistance.

REFERENCES

Acharya, K. R., Stuart, D. I., Walker, N. P. C., Lewis, M., & Phillips, D. C. (1989) *J. Mol. Biol. 208*, 99–127.
Bladen, H. A., Nylen, M. U., & Glenner, G. G. (1966) *J. Ultrastruct. Res. 14*, 449–459.
Bosch, R., Jung, G., & Winter, W. (1983) *Acta Crystallogr., Sect. C: Cryst. Struct. Commun. C39*, 776–778.
Brahms, S., & Brahms, J. (1980) *J. Mol. Biol. 138*, 149–178.
Byler, D. M., & Susi, H. (1986) *Biopolymers 25*, 469–487.
Cathcart, E. S., Comerford, I. R., & Cohen, A. S. (1965) *N. Engl. J. Med. 273*, 143–146.
Caughey, B. W., Dong, A., Bhat, K. S., Ernst, D., Hayes, S. F., & Caughey, W. S. (1991) *Biochemistry 30*, 7672–7680.
Chen, Y.-H., Yang, J. T., & Martinez, H. M. (1972) *Biochemistry 11*, 4120–4131.
Coe, J. E. (1983) *Contemp. Top. Mol. Immunol. 9*, 211–238.
Coe, J. E., & Ross, M. J. (1983) *J. Exp. Med. 157*, 1421–1433.
Coe, J. E., & Ross, M. J. (1985) *J. Clin. Invest. 76*, 66–74.
Coe, J. E., & Ross, M. J. (1990) *J. Exp. Med. 171*, 1257–1267.
Coe, J. E., Margossian, S. S., Slayter, H. S., & Sogn, J. A. (1981) *J. Exp. Med. 153*, 977–991.
Coffee, C. J., & Bradshaw, R. A. (1973) *J. Biol. Chem. 248*, 3305–3312.
Dang, C. V., Ebert, R. F., & Bell, W. R. (1985) *J. Biol. Chem. 260*, 9713–9719.
Dong, A., Huang, P., & Caughey, W. S. (1990) *Biochemistry 29*, 3303–3308.
Dong, A., Huang, P., & Caughey, W. S. (1992) *Biochemistry 31*, 182–189.
Dowton, S. B., & Holden, S. N. (1991) *Biochemistry 30*, 9531–9538.
Dowton, S. B., Woods, D. E., Mantzouranis, E. C., & Colten, H. R. (1985) *Science 228*, 1206–1208.
Etlinger, H. M., & Coe, J. E. (1986) *Int. Arch. Allergy Appl. Immunol. 81*, 189–191.
Garnier, J., Osguthorpe, D. J., & Robson, B. (1978) *J. Mol. Biol. 120*, 97–120.
Gorga, J. C., Dong, A., Manning, M. C., Woody, R. W., Caughey, W. S., & Strominger, J. L. (1989) *Proc. Natl. Acad. Sci. U.S.A. 86*, 2321–2325.
Gotschlich, E. C., & Edelman, G. M. (1967) *Proc. Natl. Acad. Sci. U.S.A. 57*, 706–712.
Greenfield, N., & Fasman, G. D. (1969) *Biochemistry 8*, 4108–4116.
Halverson, K., Fraser, P. E., Kirschner, D. A., & Lansbury, P. T., Jr. (1990) *Biochemistry 29*, 2639–2644.
Hennessey, J. P., Jr., & Johnson, W. C., Jr. (1981) *Biochemistry 20*, 1085–1094.
Hooker, T. M., Jr., & Schellman, J. A. (1970) *Biopolymers 9*, 1319–1348.
Hu, S.-T., Miller, S. M., & Samds, D. (1986) *Biochemistry 25*, 7834–7839.
Johnson, W. C., Jr. (1990) *Proteins: Struct., Funct., Genet. 7*, 205–214.
Kalb, A. J., & Livitzki, A. (1968) *Biochem. J. 109*, 669–672.

Kaplan, M. H., & Volanakis, J. E. (1974) *J. Immunol. 112*, 2135–2147.
Kilpatrick, J. M., Kearney, J. F., & Volanakis, J. E. (1982) *Mol. Immunol. 19*, 1159–1165.
Kinoshita, C. M., Ying, S.-C., Hugli, T. E., Siegel, J. N., Potempa, L. A., Houghten, R. A., & Gewurz, H. (1989) *Biochemistry 28*, 9840–9848.
Koenig, J. L., & Tabb, D. L. (1980) in *NATO Adv. Study Inst., Ser. C 57*, 241–255.
Kretsinger, R. H. (1980) *CRC Crit. Rev. Biochem. 8*, 119–174.
Kretsinger, R. H., & Nockolds, C. E. (1973) *J. Biol. Chem. 248*, 3313–3326.
Kretsinger, R. H., Tolbert, D., Nakayama, S., & Pearson, W. (1991) in *Novel Calcium-Binding Proteins* (Heizmann, C. W., Ed.) pp 17–37, Springer-Verlag, New York.
Krimm, S., & Bandekar, J. (1986) *Adv. Protein Chem. 38*, 181–364.
Liu, T.-Y., Robey, F. A., & Wang, C.-M. (1982) *Ann. N.Y. Acad. Sci. 389*, 151–160.
Mahoney, W. C., Hogg, R. W., & Hermodson, M. A. (1981) *J. Biol. Chem. 256*, 4350–4356.
Manning, M. C., & Woody, R. W. (1989) *Biochemistry 28*, 8609–8613.
Mantzouranis, E. C., Dowton, S. B., Whitehead, A. S., Edge, M. D., Bruns, G. A. P., & Colten, H. R. (1985) *J. Biol. Chem. 260*, 7752–7756.
McPhalen, C. A., Strynadka, N. C. J., & James, M. N. G. (1991) *Adv. Protein Chem. 42*, 77–144.
Miyazawa, T., & Blout, E. R. (1961) *J. Am. Chem. Soc. 83*, 712–719.
Mole, J. E., Beaulieu, B. L., Geheran, C. A., Carnazza, J. A., & Anderson, J. A. (1988) *J. Immunol. 141*, 3642–3646.
Nguyen, N. Y., Suzuki, A., Cheng, S.-M., Zon, G., & Liu, T.-Y. (1986a) *J. Biol. Chem. 261*, 10450–10455.
Nguyen, N. Y., Suzuki, A., Boykins, R. A., & Liu, T.-Y. (1986b) *J. Biol. Chem. 261*, 10456–10465.
Oliveira, E. B., Gotschlich, E. C., & Liu, T.-Y. (1979) *J. Biol. Chem. 254*, 489–502.
Osmand, A. P., Friedenson, B., Gewurz, H., Painter, R. H., Hofmann, T., & Shelton, E. (1977) *Proc. Natl. Acad. Sci. U.S.A. 74*, 739–743.
Painter, R. H., De Escallon, I., Massey, A., Pinteric, L., & Stern, S. B. (1982) *Ann. N.Y. Acad. Sci. 389*, 199–215.
Shamala, N., Nagaraj, R., & Balaram, P. (1977) *Biochem. Biophys. Res. Commun. 79*, 292–298.
Smith, G. D., Pletnev, V. Z., Duax, W. L., Balasubramanian, T. M., Bosshard, H. E., Czerwinski, E. W., Kendrick, N. E., Mattews, F. S., & Marshall, G. R. (1981) *J. Am. Chem. Soc. 103*, 1493–1501.
Susi, H., & Byler, D. M. (1986) *Methods Enzymol. 130*, 290–311.
Susi, H., & Byler, D. M. (1987) *Arch. Biochem. Biophys. 258*, 465–469.
Venyaminov, S. Y., & Kalnin, N. N. (1990) *Biopolymers 30*, 1243–1257.
Volanakis, J. E., & Kearney, J. F. (1981) *J. Exp. Med. 153*, 1604–1614.
Vyas, N. K., Vyas, M. N., & Quiocho, F. A. (1987) *Nature 327*, 635–638.
Vyas, N. K., Vyas, M. N., & Quiocho, F. A. (1991) in *Novel Calcium-Binding Proteins* (Heizmann, C. W., Ed.) pp 403–423, Springer-Verlag, New York.
Whitehead, A. S., & Rits, M. (1989) *Biochem. J. 263*, 25–31.
Whitehead, A. S., Zahedi, K., Rits, M., Mortensen, R. F., & Lelias, J. M. (1990) *Biochem. J. 266*, 283–290.
Woo, P., Korenberg, J. R., & Whitehead, A. S. (1985) *J. Biol. Chem. 260*, 13384–13388.
Young, N. M., & Williams, R. E. (1978) *J. Immunol. 121*, 1893–1898.

Registry No. PC, 107-73-3; Ca^{2+}, 7440-70-2.